Iranian Journal of Astronomy and Astrophysics
Vol. 10, No. 1, Winter 2023, 1–10
©Available online at http://ijaa.du.ac.ir
DOI: 10.22128/ijaa.2023.710.1153
Online ISSN: 2383–403X

Iranian Journal of Astronomy and Astrophysics

Research Paper

Reconstructing a Helical Magnetic Field in the Solar Corona using Lagrange Multiplier Technique

Nasim IldarTanha[1] · Sadollah Nasiri*[2]

[1] Institute for Advanced Studies in Basic Sciences (IASBS) P.O. Box 45137-66731, Zanjan, Iran;
email: n.ildartanha@gmail.com

[2] Department of Physics, Shahid Beheshti University, 1983969411, Tehran, Iran;
*email: nasiri@iasbs.ac.ir

Received: 15 August 2023; **Accepted:** 13 September 2023; **Published:** 30 September 2023

Abstract. We aim to reconstruct a nonlinear force-free magnetic field by minimizing the global departure of an initial field from a force-free and solenoidal state in the presence of helicity to obtain an appropriate representation of the magnetic field compatible with the solar coronal condition. Following the Wheatland et al method, we modify their functional to include the magnetic helicity using the Lagrange Multiplier Technique. We reconstruct the magnetic field by minimizing the new functional in a computational box whose lower side coincides with the artificial magnetogram on the photosphere while the lateral and top sides extends up to the corona and by assuming appropriate boundary conditions for the Lagrange multiplier. The artificial magnetogram is obtained by Low and Lou semi-analytical solutions. A potential field as well as a suitable ansatz is used for the initial input magnetic filed and Lagrange multiplier for the iteration procedure, respectively. The results obtained by different optimization methods are in agreement with those obtained by our approach.

Keywords: Sun, Magnetic Field, Helicity, Lagrange Multiplier

1 Introduction

The magnetic field governs the formation and dynamics of the structures in the solar corona. Hence, the measurements of the magnetic field, if possible, helps us to study the physical phenomena occurring in the corona. However, it is not possible to measure the coronal magnetic field directly by existing tools; therefore, several methods have been proposed to extrapolate the photospheric magnetic field up to the solar corona. These extrapolation methods aim to estimate the magnetic field in the corona based on the measurements of the magnetic field on the solar photosphere, known as magnetograms. The Non-Linear Force-Free Field (NLFFF) extrapolation method is one of the commonly used techniques for this purpose. For negligible non-magnetic forces, the force-free field is defined as vanishing the Lorentz force

$$(\vec{\nabla} \times \vec{B}) \times \vec{B} = 0. \tag{1}$$

* *Corresponding author*

Equation (1) is nonlinear, in general, and could be rewritten as

$$\vec{\nabla} \times \vec{B} = \alpha \vec{B}. \tag{2}$$

Using the solenoidal condition

$$\vec{\nabla}.\vec{B} = 0, \tag{3}$$

and taking the divergence of equation (2) one gets

$$\vec{B}.\vec{\nabla}\alpha(r) = 0, \tag{4}$$

which means that $\alpha(r)$ remains constant along the magnetic field lines. By the coronal conditions, in which the non-magnetic forces may be ignored, it seems that the force free model is applicable to the coronal magnetic field. To get a force-free magnetic field inside the computational box in the corona, it has to fulfill the vanishing of net force and torque on the boundary ([1–3]). A special class of force-free solutions is the potential and the linear force-free field which are obtained when α is zero or constant along the magnetic field lines, respectively. Due to the nonlinear behavior and complicated nature of the above equations, the possible analytic solutions are limited. To obtain numerical solutions for the nonlinear coronal magnetic fields, the computational codes use different methods such as the MHD relaxation (Chodura and Schluter [4]) and Grad-Rubin (Grad and Rubin [5], Sakurai [6]), upward integration [7], boundary-element (Yan and Sakurai [8]), Euler potentials ([9,10]) and optimization [11], methods. It is shown that important factors such as reliability of the solutions, fulfillment of $\nabla \times B$ and $\nabla \cdot B$ conditions, computing and converging speed, field connectivity, magnetic energy, alignment of field lines with currents, etc., are better satisfied with optimization methods (see [12,13]).

We are interested in following the Wheatland (WRS) method to reconstruct a nonlinear magnetic field by considering the effect of the magnetic helicity. Here, the Lagrange Multiplier Technique is used to add the magnetic helicity to the functional previously employed by the WRS method and to reconstruct the coronal magnetic field using an artificial photospheric magnetogram.

2 Method: Optimiztion Method in the Presence of Helicity

The Lagrange Multiplier Method is used to reconstruct a nonlinear force-free magnetic field dy adding the helicity term to the functional considered first by WRS optimization method. Let us give a very short review of the Wheatland et al [11] who proposed a new optimization method for reconstructing a force-free magnetic fields using their boundary values in the computational box with its lower side located on the solar photosphere. They solved the resultant equation by an iterative procedure and optimized the global departure of an initial field from a force-free and solenoidal state by introducing the following functional

$$L_W = \int_v \vec{\Omega}_W^2 \vec{B}^2 dv, \tag{5}$$

where

$$\vec{\Omega}_W = B^{-2}[(\vec{\nabla} \times \vec{B}) \times \vec{B} - (\vec{\nabla} \cdot \vec{B})\vec{B}]. \tag{6}$$

By defining

$$\vec{F}_W = \vec{\nabla} \times (\vec{\Omega} \times \vec{B}) - \vec{\Omega} \times (\vec{\nabla} \times \vec{B}) - \vec{\nabla}(\vec{\Omega} \cdot \vec{B}) + \vec{\Omega}(\vec{\nabla} \cdot \vec{B}) + \vec{\Omega^2}\vec{B}, \tag{7}$$

and

$$\vec{G}_W = \hat{n} \times (\vec{\Omega} \times \vec{B}) - \hat{n}(\vec{\Omega} \cdot \vec{B}), \tag{8}$$

and differentiating equation (5) with respect to t one gets

$$\frac{1}{2}\frac{dL_W}{dt} = -\int \frac{\partial \vec{B}}{\partial t}.\vec{F}_W dv - \int \frac{\partial \vec{B}}{\partial t} \cdot \vec{G}_W d\vec{S}. \tag{9}$$

Assuming the following boundary condition

$$\frac{\partial \vec{B}}{\partial t}|_s = 0, \tag{10}$$

the equation (9) becomes

$$\frac{dL_W}{dt} = -2\int \mu \vec{F}_W^2 dv, \tag{11}$$

which is always negative. This means that L_W will decrease as the iteration process goes on. Since L_W is always positive, then L_W will approach to zero at the end of the iteration giving the force-free and divergence-free magnetic field everywhere in the computational box through the following iteration equation

$$\frac{\partial \vec{B}}{\partial t} = \mu \vec{F}_W, \tag{12}$$

where μ is a positive constant.

Here, we follow the Nasiri et al [14] and Fatholahzadeh et al [15] and generalize the functional of WRS to include the total magnetic helicity. Magnetic helicity is a measure of the topological structure of the magnetic field. It is a measure of the twistedness or linkage of magnetic field lines and plays a vital role in the dynamics of the solar eruptions and occurrence of the flare phenomena. By including the helicity term in the optimization functional, one may argue that the resulting extrapolated magnetic field can better represent the observed coronal features. The magnetic helicity is defined as follows

$$H = \int \vec{A} \cdot \vec{B} dv, \tag{13}$$

where $\vec{A}$ is magnetic vector potential and v is the plasma volume of the computational box. The concept of magnetic helicity as a conserved quantity has recently become important (especially since magnetic helicity conserves better than the magnetic energy through the magnetic re-connection processes) (Ashwanden [16], Woltjer [17] and Buniy [18]). Under a gauge transformation that replaces $\vec{A}$ by $\vec{A} + \vec{\nabla} g$, where g is an arbitrary real-valued function, the magnetic helicity H changes as

$$H \to H + \int g(\hat{n} \cdot \vec{B}) d\vec{S}. \tag{14}$$

Which means that H is not a gauge invariant quantity. However, in optimization procedure, we will differentiate H with respect to iteration parameter t and get

$$\frac{\partial H}{\partial t} \to \frac{\partial H}{\partial t} + \int g(\hat{n} \cdot \frac{\partial \vec{B}}{\partial t}) d\vec{S}. \tag{15}$$

Using equation (10), the second term vanishes so H will remain as a gauge invariant quantity. To construct our functional L_{new}, we use the Lagrange multiplier, Λ, to enforce the helicity as follows

$$L_{new} = \int \vec{B}^2 \vec{\Omega}^2 dv + \int \Lambda(\vec{A} \cdot \vec{B}) dv, \tag{16}$$

here the $\vec{\Omega}$ has the same form

$$\vec{\Omega}_W = B^{-2}[(\vec{\nabla} \times \vec{B}) \times \vec{B} - (\vec{\nabla} \cdot \vec{B})\vec{B}], \tag{17}$$

as in WRS [11]. In the same manner as done by WRS [11] one may differentiate L_{new} with respect to t to get

$$\frac{1}{2}\frac{dL}{dt} = -\int \frac{\partial \vec{B}}{\partial t}.\vec{F}_{new} dv - \int \frac{\partial \vec{B}}{\partial t} \cdot \vec{G}_{new} d\vec{S} + \frac{1}{2}\int \frac{\partial \Lambda(r,t)}{\partial t}(\vec{A} \cdot \vec{B}) dv, \tag{18}$$

where

$$\vec{F}_{new} = \vec{\nabla} \times (\vec{\Omega} \times \vec{B}) - \vec{\Omega} \times (\vec{\nabla} \times \vec{B}) - \vec{\nabla}(\vec{\Omega} \cdot \vec{B}) + \vec{\Omega}(\vec{\nabla} \cdot \vec{B}) + \vec{\Omega}^2 \vec{B} - \Lambda(r,t)\vec{A}, \tag{19}$$

$$\vec{G}_{new} = \hat{n} \times (\vec{\Omega} \times \vec{B}) - \hat{n}(\vec{\Omega} \cdot \vec{B}) - \hat{n} \times \Lambda(r,t)\vec{A}. \tag{20}$$

By assuming

$$\frac{\partial \vec{B}}{\partial t} = \mu_1 \vec{F}_{new}, \tag{21}$$

and

$$\frac{1}{2}\frac{\partial \Lambda(r,t)}{\partial t} = -(\vec{A} \cdot \vec{B}), \tag{22}$$

and using the boundary conditions

$$\frac{\partial \vec{B}}{\partial t}|_s = \frac{\partial \vec{A}}{\partial t}|_s = 0. \tag{23}$$

One gets the decreasing condition for L_{new} as follows

$$\frac{dL_{new}}{dt} = -2\int \mu_1 \vec{F}^2_{new} dv - 2\int \mu_2 (\vec{A}.\vec{B})^2 dv, \tag{24}$$

where μ_1 and μ_2 are positive constants.
According to equation (19), since $\vec{F}$ depends on $\vec{A}$ it seems that $\vec{F}$ is gauge dependent, while, having a unique magnetic field in each iteration steps of reconstruction, $\vec{F}$ must be a gauge independent quantity. However, the appearance of Λ and $\vec{A}$ in the multiple form in equation (19), may serve to make the combined form of $\Lambda(r,t)\vec{A}$ as a gauge independent quantity, although, each one of the Λ and $\vec{A}$ are gauge dependent. This can be deduced from boundary condition equation (23), in which

$$\vec{F}_{new}|_s = 0. \tag{25}$$

Thus,

$$\Lambda(r,t)\vec{A} = \vec{\nabla} \times (\vec{\Omega} \times \vec{B}) - \vec{\Omega} \times (\vec{\nabla} \times \vec{B}) - \vec{\nabla}(\vec{\Omega} \cdot \vec{B}) + \vec{\Omega}(\vec{\nabla} \cdot \vec{B}) + \vec{\Omega}^2 \vec{B}, \tag{26}$$

on the surface. By equation (7), the right hand of equation (26) is $\vec{F}_W$; thus,

$$\Lambda(r,t)\vec{A} = \vec{F}_W, \tag{27}$$

or

$$\Lambda(r,t) = \frac{\vec{F}_W \cdot \vec{B}}{\vec{A} \cdot \vec{B}}. \tag{28}$$

By equations (22) and (28) we see that Λ depends on $\vec{A}$. Therefore, Λ and $\vec{A}$ both are arbitrary quantities. However, by equation (27), $\Lambda(r,t)\,\vec{A}$ which is equal to $\vec{F}_W$ must be gauge independent. Note that two vital prerequisites should be considered while Λ is satisfied by equation (28): Its dimension should be consistent in equation (16), and it must be satisfied by both equations (22) and (28). Therefore, substituting for $A.B$ from equation (28), as a guideline equation, in equation (22), one gets the following evolution equation for Λ.

$$\frac{\partial \Lambda^2(r,t)}{\partial t} = (\vec{F}_W \cdot \vec{B})^2. \tag{29}$$

Starting with a potential field as an input and iterating the equations (21) and (29), one may update both of the magnetic field and Lagrange Multiplier, simultaneously, needless of input for $\vec{A}$. Finally, by making L_{new} stationary, one may obtain the force-free field in the computational box.
In the next sections, we apply the method to an artificial magnetogram and deliver the corresponding results.

3 Results

3.1 Application to an Example Magnetogram

The magnetic field at any point in space is a vector quantity. The appropriate magnetogram is obtained for different components of the magnetic field from the solution of the Low and Lou semi-analytic model [19] and the results are shown in Figure 1 for Bx, By, and Bz, as the three components of the magnetic field. We use the resulting magnetogram and reconstruct the magnetic field lines by our model and compare them with those obtained by the corresponding Low and Lou solutions. The results are plotted in Figure (2).

3.2 Figures of Merit

Figures of merit are numerical expressions taken to represent the quality of the performance or efficiency of a given procedure [20]. Here, we use it to quantify the degree of agreement between vector fields B (for the input model field) and b (the NLFF model solutions) specified on identical sets of grid points. We use five metrics that compare either local characteristics (e.g., vector magnitudes and directions at each grid point), or the global energy content in addition to the force and divergence integrals as defined in Schrijver et al. [21]. The vector correlation C_{vec} metric analogous the standard correlation coefficient for the scalar functions is given by

$$C_{vec} = \frac{\Sigma_i B_i \cdot b_i}{(\Sigma_i |b_i|^2 \cdot \Sigma_i |B_i|^2)^{\frac{1}{2}}}, \tag{30}$$

where B_i and b_i are the vectors at each point i. If the vector fields are identical, then $C_{vec} = 1$, if $B_i \perp b_i$, then $C_{vec} = -1$.
The second metric, C_{cs} is based on the Cauchy-Schwarz inequality ($\mid a \cdot b \mid \leq \mid a \mid\mid b \mid$ for any two vectors a and b)

$$C_{cs} = \frac{1}{M} \Sigma_i \frac{B_i \cdot b_i}{\mid B_i \mid\mid b_i \mid} = \frac{1}{M} \Sigma_i cos\theta_i, \tag{31}$$

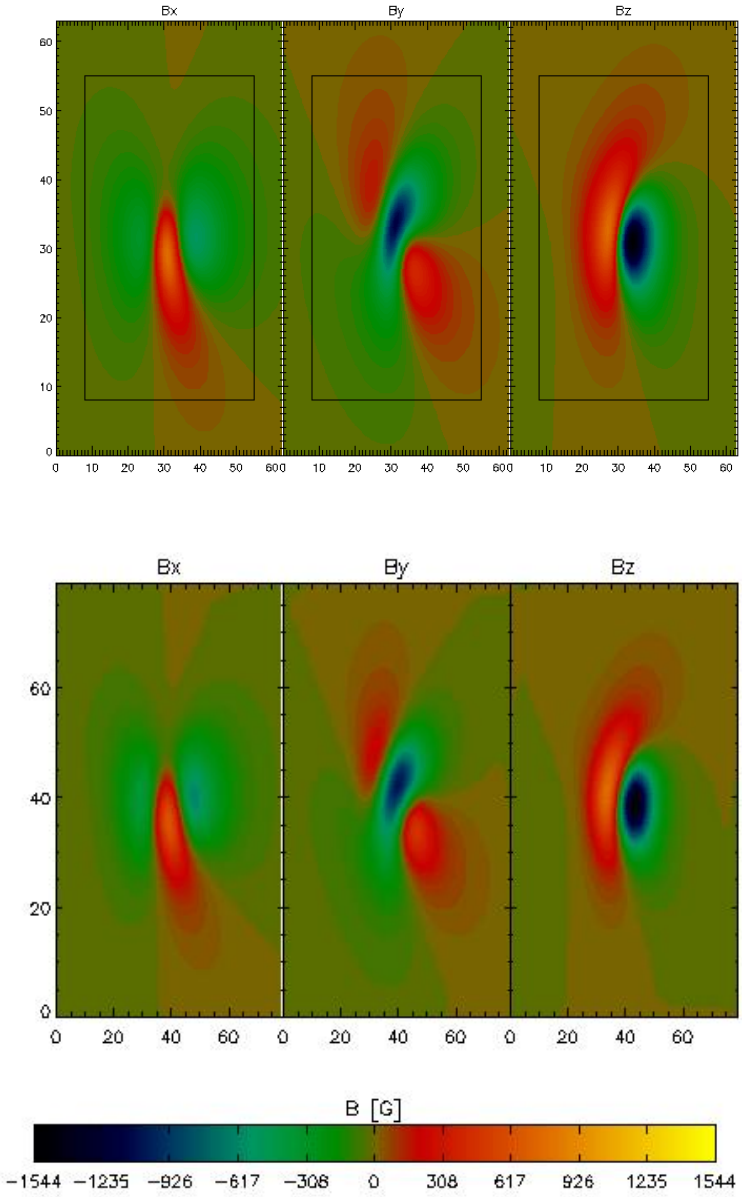

Figure 1: From left to right the x, y and z components of the vector magnetogram of Low and Lou solution. The first row shows the original vector magnetogram inferred from the Low and Lou solution. In the second row we applied preprocessing to the original vector magnetogram using the preprocessing scheme of Wiegelmann et al. [20]

Table 1: Quality comparison of NLFFF field obtained by WRS and Lagrange multiplier methods (Nasiri et al and this paper), for a computational box with grid numbers: $nx = 80$, $ny = 80$, $nz = 20$

Models	**Low& Lou**	**WRS**	**Nasiri et al**	**This paper**
ϵ	1.0	$1 \cdot 5353$	$1 \cdot 0853$	$1 \cdot 0794$
E_m	0.0	·5567	·0539	·0668
C_{vec}	1.0	·8609	·9452	·920513
E_n	0.0	·5836	·0909	·1138
C_{cs}	1.0	·8988	·9434	·9597

where M is the total number of vectors in the volume, and $\theta_i$the angle between input and model magnetic fields at point i . This metric is mostly a measure of the angular differences of the vector fields: $C_{cs} = 1$ when B and b are parallel and $C_{cs} = -1$ if they are anti-parallel; $C_{cs} = 0$ if $B_i \perp b_i$ at each point.

Next, we introduce two measures for the vector errors, one by normalizing to the average vector norm, another by averaging over relative differences. The normalized vector error E_n is defined as

$$E_n = \frac{\Sigma_i \mid b_i - B_i \mid}{\Sigma_i \mid B_i \mid}, \tag{32}$$

The mean vector error E_m is defined as

$$E_m = \frac{1}{M} \Sigma_i \frac{|b_i - B_i|}{|B_i|}. \tag{33}$$

Unlike the first two metrics, the perfect agreement between the two vector fields results in $E_n = E_m = 0$.
we are also interested in determining how well the models estimate the energy contained in the field. Thus, we use the total magnetic energy in the model field normalized to the total magnetic energy in the input field as a global measure of the quality of the fit

$$\epsilon = \frac{\Sigma_i \mid b_i \mid^2}{\Sigma_i \mid B_i \mid^2}, \tag{34}$$

where $\epsilon = 1$ is for the best agreement between the model field and the nonlinear force-free model solutions.

We calculate the above relations for 5000 iteration steps and the results are shown for Low and Lou analytic solutions as well as for WRS and Nasiri et al [14] models for the same number of iteration steps and the corresponding magnetic fields are reconstructed. These parameters for different methods are tabulated in Table 1. As it is seen in the table, all metrics of Lagrange multiplier models (both Nasiri et al and this paper) are in better agreement with Low and Lou analytical method compared with those of WRS model.

A few magnetic field lines are reconstructed for the models given by Low and Lou, WRS, Nasiri et al and this paper, on the artificial magnetograms obtained by using the Low and Lou analytical solutions and the results are shown in Figure (2). The same as numerical metrics of Table (1), the results obtained by different methods are in agreement with analytical approach.

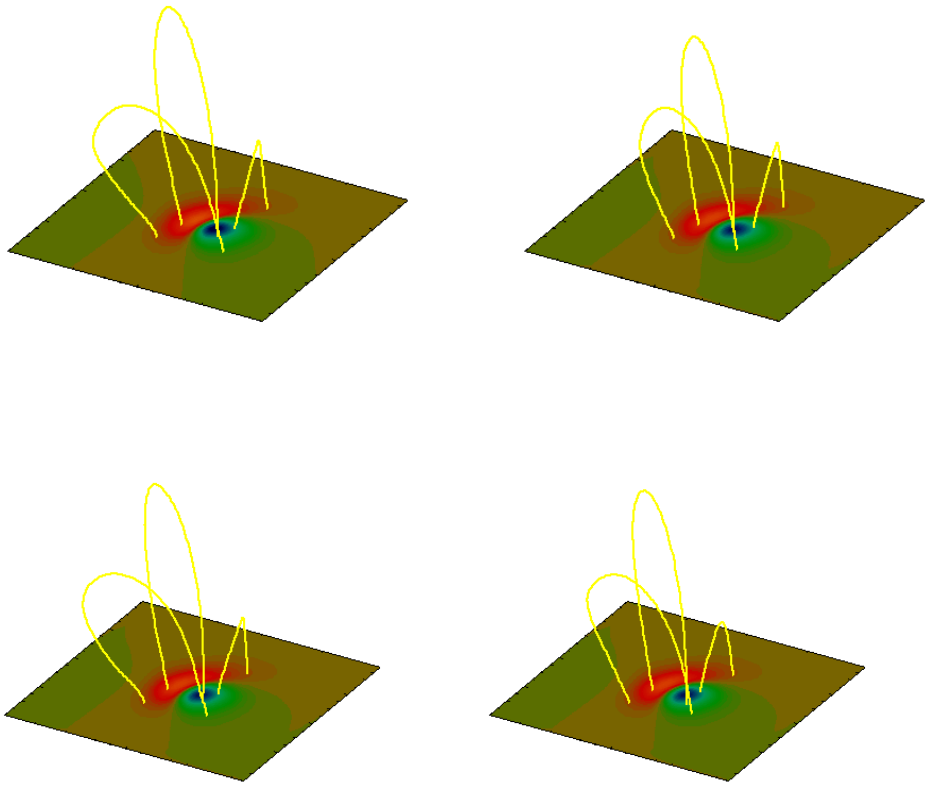

Figure 2: Some field lines reconstructed on the Low and Lou artificial magnetograms: Low and Lou analytical method (top left), WRS (top right), Nasiri et al (bottom left) and this paper (bottom right).

4 Conclusions and Outlook

Within this work, we used a constrained optimization method using the Lagrange Multiplier Technique to reconstruct a nonlinear force-free magnetic field. This is done by assuming the helicity as a constraint on the force-free and the divergence free magnetic field. Due to certain boundary conditions applied to the magnetic field and the Lagrange Multiplier on the surface of the computational box, and by assuming an appropriate expression for the input Lagrange Multiplier, the gauge dependence of the helicity is removed and the nonlinear force-free magnetic field is reconstructed by iterating the evolution equations for the magnetic field and the Lagrange multiplier. To compare the results, the values of the different metrics such as the mean vector error, relative energy, etc., are shown in Table (1), as well as the magnetic field lines are reconstructed and plotted for different models in Figure (2). For the future work, the present model may be applied to a real magnetogram and deduce the energetic and the dynamics of the flaring phenomena in the active regions of the solar corona.

Authors' Contributions

All authors have the same contribution.

Data Availability

No data available.

Conflicts of Interest

The authors declare that there is no conflict of interest.

Ethical Considerations

The authors have diligently addressed ethical concerns, such as informed consent, plagiarism, data fabrication, misconduct, falsification, double publication, redundancy, submission, and other related matters.

Funding

This research did not receive any grant from funding agencies in the public, commercial, or nonprofit sectors.

References

[1] Molodensky, M. M. 1974, Sol. Phys., 39, 393.

[2] Molodensky, M. M. 1969, Soviet Astronomy, 12, 585.

[3] Aly, J. J. 1989, Sol. Phys., 120, 19.

[4] Chodura, R. & Schlueter, A. 1981, J. Comput. Phys., 41, 68.

[5] Grad, H. & Rubin, H. 1958, Proc. Second UN Int. Atomic Energy Conference, 31 (Geneva: UN).

[6] Sakurai, T. 1981, Sol. Phys., 69, 343.

[7] Nakagawa, Y. & Tanaka, K. 1974, ApJ, 190, 711.

[8] Yan, Y. & Sakurai, T. 2000, Sol. Phys., 195, 89.

[9] Stern, D. P. 1966, Space Sci. Rev., 6, 147.

[10] Parker, E. N. 1979, Cosmical magnetic fields: Their origin and their activity, Oxford, Clarendon Press; New York, Oxford University Press, 858.

[11] Wheatland, M. S., Sturrock, P. A. & Roumeliotis, G. 2000, ApJ, 540, 1150.

[12] Schrijver, C. J., De Rosa, M. L., Metcalf, T. R., Liu, Y., McTiernan, & et al. 2006, Sol. Phys., 235, 161.

[13] Schrijver, C. J., DeRosa, M. L., Metcalf, T., Barnes, G., Lites, B., Tarbell, T., McTiernan, & et al. 2008, ApJ, 675, 1637.

[14] Nasiri, S. & Wiegelmann, T. 2019, J. Atmos. & Sol. Terr. Phys., 1882, 181.

[15] Fatholahzadeh, S., Jafarpour, M. H. & Nasiri, S. 2023, A & A.

[16] Aschwanden, M. 2000, Physics of the Solar Corona An Introduction with Problems and Solutions, Springer-Verlag, Berlin, Heidelberg.

[17] Woltjer, L. 1958, Proceedings of the Natl. Acad. Sci., 44, 489.

[18] Buniy, R. V. & Kephart, T. W. 2014, Ann. Phys., 344.

[19] Low, B. C. & Lou, Y. Q. 1990, ApJ, 352, 343.

[20] Wiegelmann, T., Inhester, B. & Sakurai, T. 2006, Sol. Phys. , 223, 215.

[21] Schrijver, C. J., De Rosa, M. L., Metcalf, T. R., Liu, Y., McTiernan, J., Régnier, S., & et al. 2006, Sol. Phys., 235, 161.